Appl Microbiol Biotechnol (2013) 97:6201–6209
DOI 10.1007/s00253-013-4922-x



# LPS–protein aggregation influences protein partitioning in aqueous two-phase micellar systems

**André Moreni Lopes · Valéria de Carvalho Santos-Ebinuma · Leticia Celia de Lencastre Novaes · João Vitor Dutra Molino · Leandro Ramos Souza Barbosa · Adalberto Pessoa Jr · Carlota de Oliveira Rangel-Yagui**

Received: 18 February 2013 / Revised: 8 April 2013 / Accepted: 10 April 2013 / Published online: 3 May 2013


**Abstract** Lipopolysaccharide endotoxins (LPS) are the most common pyrogenic substances in recombinant peptides and proteins purified from Gram-negative bacteria, such as *Escherichia coli*. In this respect, aqueous two-phase micellar systems (ATPMS) have already proven to be a good strategy to purify recombinant proteins of pharmaceutical interest and remove high LPS concentrations. In this paper, we review our recent experimental work in protein partitioning in Triton X-114 ATPMS altogether with some new results and show that LPS–protein aggregation can influence both protein and LPS partitioning. Green fluorescent protein (GFPuv) was employed as a model protein. The ATPMS technology proved to be effective for high loads of LPS removal into the micelle-rich phase (%$REM_{LPS}$>98 %) while GFPuv partitioned preferentially to the micelle-poor phase ($K_{GFPuv}$<1.00) due to the excluded-volume interactions. However, theoretically predicted protein partition coefficient values were compared with experimentally obtained ones, and good agreement was found only in the absence of LPS. Dynamic light scattering measurements showed that protein–LPS interactions were taking place and influenced the partitioning process. We believe that this phenomenon should be considered in LPS removal employing any kind of aqueous two-phase system. Nonetheless, ATPMS can still be considered as an efficient strategy for high loads of LPS removal, but being aware that the excluded-volume partitioning theory available might overestimate partition coefficient values due to the presence of protein–LPS aggregation.

**Keywords** Protein–LPS interaction · Aqueous two-phase micellar system · LPS removal · Dynamic light scattering

A. M. Lopes (✉) · V. d. C. Santos-Ebinuma · L. C. d. L. Novaes · J. V. D. Molino · A. Pessoa Jr
Department of Biochemical and Pharmaceutical Technology, School of Pharmaceutical Sciences, University of São Paulo-FCF/USP, Av. Prof. Lineu Prestes, 580, B16 Cidade Universitária, 05508-000 São Paulo, SP, Brazil
e-mail: andreml@usp.br

L. R. S. Barbosa
Department of General Physics, Institute of Physics-University of São Paulo, São Paulo, Brazil

C. d. O. Rangel-Yagui
Department of Pharmacy, School of Pharmaceutical Sciences, University of São Paulo-FCF/USP, São Paulo, Brazil

## Introduction

In the last four decades, the scientific community experienced a major change in the biotechnology field, driven by the advent of genetic engineering, i.e., the direct transfer of DNA from one organism to another. Such manipulation was accomplished for the first time in 1973 by Herbert Boyer and Stanley Cohen. As a result, recombinant DNA technology altogether with molecular biology has opened up numerous possibilities for the large-scale production of many biomolecules of pharmaceutical and technological interest (Primrose and Twyman 2006). In spite of all the advances in this field, recombinant biomolecules are still mostly expressed in the *Escherichia coli* bacteria, which is the first microorganism employed by Boyer and Cohen (Lopes et al. 2012; Chen 2012; Terpe 2006). However, this microorganism presents contaminants, such as lipopolysaccharide endotoxins (LPS), which are one of the major components of the outer membrane of Gram-negative bacteria.

LPS are the most common pyrogenic substances in recombinant peptides and proteins purified from *E. coli*

(Anspach 2001). Due to the toxic effect on humans, it is essential to remove LPS from injectable drug preparations and other biological and pharmaceutical products. In this sense, liquid–liquid extraction such as aqueous two-phase micellar systems (ATPMS) can be a powerful alternative to purify recombinant proteins of pharmaceutical interest and remove high LPS concentrations (Lopes et al. 2010, 2011; Magalhães et al. 2007).

ATPMS for separation and purification of proteins and other biomolecules have been of paramount importance for many advances in the biotechnology industry (Fischer et al. 2012; Gupta et al. 2004). These systems are based on the property that some micellar solutions present to phase separate into a micelle-rich and a micelle-poor phase, under certain conditions (Liu et al. 1996). For example, upon increasing the temperature, an aqueous solution of the nonionic surfactant octylphenol ethoxylate, Triton™ X-114 (TX-114), undergoes into a macroscopic phase separation into a top, micelle-poor phase and a bottom, micelle-rich phase, as schematically shown in Fig. 1 (Lopes et al. 2010; Nikas et al. 1992). Based on this difference in the physicochemical environment of the two coexisting micellar phases, and since both phases contain about 60 to 90 % of water, ATPMS provides a powerful alternative for protein purification (Liu et al. 1996).

The partitioning behavior of a protein in an ATPMS can be quantified in terms of the protein partition coefficient, defined as follows:

$$K_{\mathrm{p}} = \frac{C_{\mathrm{p,\ bottom}}}{C_{\mathrm{p,\ top}}} \tag{1}$$

where $C_{p,\ \mathrm{bottom}}$ and $C_{p,\ \mathrm{top}}$ are the protein concentrations in the bottom, micelle-rich phase and in the top, micelle-poor phase, respectively. The partitioning behavior of hydrophilic proteins in an ATPMS composed of cylindrical micelles was modeled by Blankschtein and coworkers (Nikas et al. 1992). Accordingly, the partitioning of proteins is governed primarily by repulsive, steric, excluded volume (EV) interactions between globular hydrophilic proteins and noncharged micelles. Based on this excluded-volume hypothesis, statistical thermodynamics was used to derive an expression for the protein partition coefficient in ATPMS. It was found that, under conditions of low protein concentration, noncharged surfactants, and low salt concentration, the partition coefficient is given by:

$$K_{\mathrm{p}}^{\mathrm{EV}} = \exp\left[-\left(\phi_{\mathrm{bottom}} - \phi_{\mathrm{top}}\right)\left(1 + \frac{R_{\mathrm{p}}}{R_0}\right)^2\right] \tag{2}$$

where $\phi_{\mathrm{bottom}}$ and $\phi_{\mathrm{top}}$ are the surfactant volume fractions in the bottom (micelle-rich) and top (micelle-poor) phases, respectively, $R_{\mathrm{p}}$ is the protein hydrodynamic radius, and $R_0$ is the cross-sectional radius of each cylindrical micelle (adapted from Lue and Blankschtein 1996; Nikas et al. 1992).

An expansion of the theory above was further proposed for systems composed of charged surfactants, in order to take into account electrostatic interactions (Kamei et al. 2002; Rangel-Yagui et al. 2003). Affinity interactions were also investigated and proven to play an important role whenever they are strong enough to overcome the excluded-volume effect (Lopes et al. 2008; Mazzola et al. 2006).

It is well known that the addition of a third component (e.g., salts) to ATPMS usually alters the possible interactions of the system, such as intra/intermicellar and biomolecule-micelle interactions (Mazzola et al. 2008). In this paper, we review our recent experimental work in LPS-containing systems (Lopes et al. 2010, 2011) altogether with some new results and show that the presence of this component results in a new phenomenon that has to be taken into account: LPS–protein aggregation. We discuss how it influences the excluded-volume model and the importance of being aware of this

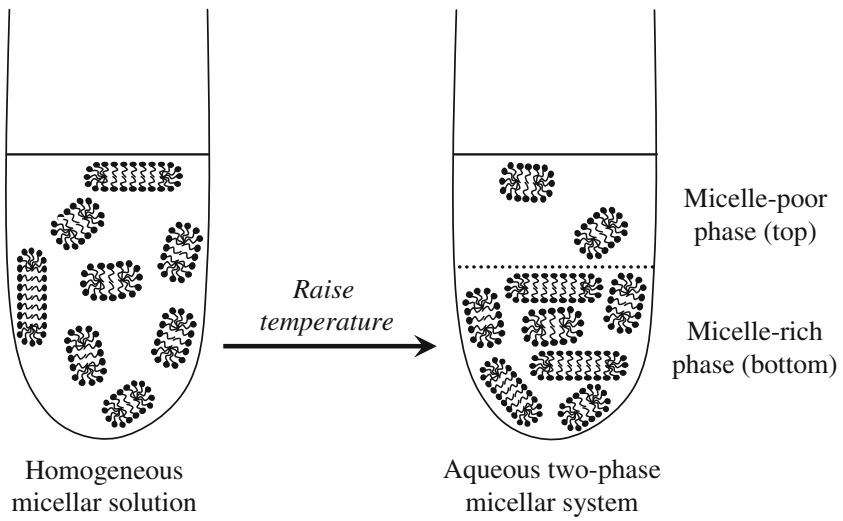


**Fig. 1** Schematic representation of an aqueous two-phase micellar system. Upon phase separation, the biomolecule can be concentrated in one of the phases according to steric, electrostatic, and/or affinity interactions. Based on Nikas et al. (1992)

interaction when theoretically planning partitioning conditions to extract/purify proteins expressed in *E. coli*. Green fluorescent protein (GFPuv) was used as a model protein.

## Materials and methods

### Materials

Nonionic surfactant octylphenol ethoxylate (TX-114) was purchased from Sigma-Aldrich® (St. Louis, MO). LPS from *E. coli* 055:B5 and kinetic chromogenic kit (LAL Kinetic-QCL®) were purchased from Cambrex (Walkersville, MD). Recombinant GFPuv was provided by Clontech (95 % purity, Palo Alto, CA). All solutions were prepared in McIlvaine's buffer, pH 7.2, consisting of 16.4 mM disodium phosphate and 1.82 mM citric acid in water purified by a Millipore Milli-Q system (Bedford, MA). The glassware used was washed in 50:50 ethanol/1 M sodium hydroxide bath, followed by a 1-M nitric acid bath, rinsed copiously with Milli-Q water and, finally, dried in oven at 250 °C for 1 h. All solution transfers were performed using LPS-free devices. Sterile, disposable plasticware was used at all times to prevent LPS contamination. The LPS concentration in the Milli-Q water was quantified and found to be below 0.05 EU/mL. All other reagents were of analytical grade and used as received.

### Determination of GFPuv concentration

GFPuv fluorescence intensity was determined in a spectrofluorometer (RF 5301 PC, Shimadzu Corporation, Kyoto, Japan) with $\lambda_{excitation}$=394 nm and $\lambda_{emission}$=509 nm. Standard solutions with different concentrations of commercial pure recombinant GFPuv were used to generate a standard curve.

### Determination of LPS concentration

Pure LPS samples added to ATPMS were obtained from *E. coli* (ATCC 25922), which was cultivated according to Westphal and Jann (1965) and purified according to Lopes et al. (2011). LPS concentration in the samples was determined by kinetic chromogenic method employing the LAL Kinetic-QCL® Kit. All sample dilutions and additions of lysate to microtiter plate wells were performed using a calibrated multichannel pipette with pyrogen-free tips. The plate-based photometric assay ($\lambda$= 405 nm) was incubated at 37.0 °C in an ELISA microplate reader (ELx808cse-BIO-TEK Instruments). The positive control was contaminated with an equal LPS concentration of 5.00 EU/mL, and the results for all tests were considered valid whenever the value of recovered LPS concentration was between 50 and 200 % of this value (US Pharmacopeia and National Formulary-USP-24-NF-19 2000). For TX-114-containing samples, surfactant interference was taken into account by subtracting the values obtained for blank assays (pure TX-114 at the same concentration of the sample) from the total value obtained for the LPS sample.

### Mapping the coexistence curve of TX-114/buffer system

Coexistence curve of the TX-114/buffer systems was mapped out in pure McIlvaine's buffer and also in the presence of $10^5$ EU/mL of LPS, by means of cloud-point measurements (Albertsson 1986; Nikas et al. 1992). Briefly, buffered surfactant solutions of known concentrations were prepared and placed in a transparent thermoregulated device (Polyscience, model 9505) with temperature control within 0.2 °C. The temperature was first lowered such that the solution exhibited a single and clear phase. Afterwards, the temperature was raised slowly and the temperature at which the solution first became cloudy, indicating the onset of phase separation, was taken as cloud point. The experimental coexistence curve was then obtained by plotting the observed cloud-point values as a function of the corresponding surfactant concentrations. The TX-114 concentration in each coexisting phase of a two-phase system can be read from the phase diagram by noting the intersections of the operating tie-line and the fitted coexistence curve. The procedure was performed in triplicate to ensure reproducibility.

### Dynamic light scattering measurements

Dynamic light scattering (DLS) measurements were performed in a Malvern ZetaSizer Nano ZS apparatus, with a HeNe (633 nm) laser. Initially, the hydrodynamic diameter of GFPuv in an 800-μL solution composed by 0.5 mg/mL GFPuv solution in phosphate buffer at pH 7.4 was measured in an acrylic dispensable cuvette at a fixed 90° angle. Subsequently, small aliquots (10 μL) of LPS solutions at 1 and 5 mg/mL, which represents an activity of $10^7$ and $5\times10^7$ EU/mL, respectively, were added to the cuvette containing the GFPuv solution, being gently mixed, and reaching equilibrium after 5 min. After this period, new measurements were performed. The data were acquired after three independent runs, being each run composed by 90 measurements. The data presented here are the average of these measurements. According to this methodology the (LPS)/(GFPuv) ratio ranges from 0 up to 1.5, where no more changes in the (LPS)/(GFPuv) complex were evidenced. The temperature was kept constant during the experiments at $T$=22.0±0.1 °C.

### Partitioning in ATPMS

Buffered systems, each with a total mass of 5.0 g, were prepared in LPS-free graduated test tubes by adding specific amounts of

surfactant (TX-114), McIlvaine buffer pH 7.2, 100 μg/mL of GFPuv standard (95 % purity, Clontech) and/or $10^7$ EU/mL of pure LPS. The systems were homogenized in an orbital shaker (Barnstead/Thermolyne, model 400110) at 8 rpm for 1 h and equilibrated at 10.0 °C, presenting a single phase. Subsequently, the systems were placed in a thermo-regulated device (Polyscience, model 9505), previously set at the desired temperature (27.0, 29.3, 33.3, 35.0, and 37.3 °C ) and kept there for 3 h to reach partition equilibrium. Afterwards, the two coexisting micellar phases formed were withdrawn separately and the concentrations of GFPuv and LPS determined in each phase.

Partitioning behavior of GFPuv in ATPMS was quantified in terms of partition coefficient, $K_{GFPuv}$, defined in Eq. 1.

Volume ratio ($R$) between the phases of the system was calculated as:

$$R = \frac{V_{bottom}}{V_{top}} \tag{3}$$

where $V_{bottom}$ and $V_{top}$ are the volumes of micelle-rich and micelle-poor phases, respectively.

The mass balance (%$MB_{GFPuv}$) was calculated according to the following equation:

$$\%MB_{GFPuv} = \left(\frac{C_{GFPuv,\ top}\ V_{top} + C_{GFPuv,bottom}\ V_{bottom}}{C_{GFPuv,\ i}\ V_i}\right)100\ \% \tag{4}$$

where $C_{GFPuv,\ top}$, $C_{GFPuv,\ bottom}$, and $C_{GFPuv,\ initial}$ are the GFPuv concentrations in the top (micelle-poor) phase, bottom (micelle-rich) phase, and in the GFPuv stock solution initially added to the system, respectively. $V_{top}$, $V_{bottom}$, and $V_{initial}$ are the volumes of the top phase, bottom phase, and the GFPuv stock solution initially added to the system, respectively.

The percentage of LPS removal in the bottom, micelle-rich phase (%$REM_{LPS}$) was also calculated, according to the following equation:

$$\%REM_{LPS} = 100 - \left(\frac{C_{LPS,\ top}\ V_{top}}{C_{LPS,\ i}\ V_{LPS,\ i}}\right)100\ \% \tag{5}$$

Where $C_{LPS,\ top}$ and $C_{LPS,\ initial}$ refer to LPS concentrations (in endotoxin units per milliliter) in the top phase and the stock solution initially added to the system, respectively. $V_{top}$ and $V_{initial}$ are the volumes of the top phase and the stock solution initially added to the system, respectively.

## Results

### Coexistence curve of the TX-114/buffer micellar system

The coexistence curve of the TX-114/buffer micellar system (Fig. 2a) was determined varying the TX-114 concentrations in McIlvaine buffer at pH 7.2 as described in the "Materials

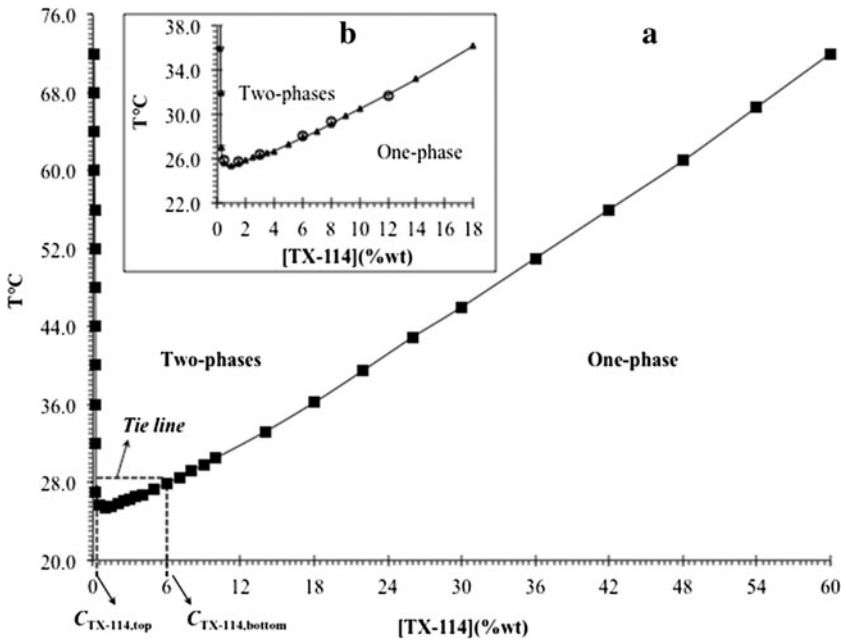


**Fig. 2** **a** Coexistence curve of the TX-114/McIlvaine buffer micellar system (*squares*). The region within the curve is the two-phase region, representing conditions under which micellar solutions separate into two macroscopic phases. The region outside the curve is the one-phase region, representing conditions under which micellar solutions correspond to homogeneous phases. The *dashed line* represents a tie-line corresponding to 28.0 °C. A TX-114 micellar solution having any TX-114 concentration along the tie-line will phase separate into top and bottom phases having concentrations $C_{TX\text{-}114,top}$=0.00 and $C_{TX\text{-}114,bottom}$=0.06 wt.%, respectively. **b** Cloud-point values (*empty circles*) obtained with addition of $10^5$ EU/mL of LPS to ATPMS. The *error bars* represent 95 % confidence levels for the measurements

and methods." It is known that the minimum point of the coexistence curve is referred as the lowest critical point, which is characterized by a critical temperature ($T_c$) and a critical surfactant concentration ($X_c$). In this work, the values obtained to these parameters were 25.4 °C and 1.00 wt.%, respectively, as can be seen in Fig. 2a. At any given temperature above $T_c$, a tie-line is obtained by drawing a parallel line to the TX-114 concentration axis.

Since the top and bottom micellar phases have densities of approximately 1 g/mL, the TX-114 weight fractions can be considered as volume fractions and, therefore, the ($\phi_{bottom}$–$\phi_{top}$) value corresponds to the tie-line length divided by 100, i.e., ($\phi_{bottom}$–$\phi_{top}$)=($C_{TX\text{-}114,\ bottom}$–$C_{TX\text{-}114,\ top}$)/100. According to Eq. (2), for a given hydrophilic protein (fixed $R_p$) and a given surfactant type (fixed $R_0$), the higher the value of ($\phi_{bottom}$–$\phi_{top}$), the lower will be $K_p$. One should keep in mind that ideally protein partitioning is better when $K_p$ approaches zero or infinite, which means that the target protein partitioned extremely to one of the phases. The coexistence curve in Fig. 2a shows that the value of ($\phi_{bottom}$–$\phi_{top}$) increases as the temperature increases. As result, $K_p$ should decrease with an increase in temperature (see Eq. (2)).

In Fig. 2b, the influence of high LPS concentrations ($10^5$ EU/mL) on the cloud point was investigated. The circles represent measurements in the presence of LPS. As can be seen, no significant difference was observed for the cloud-point values obtained in the presence of LPS.

## GFPuv partitioning in TX-114/buffer micellar system

In order to investigate LPS influence in protein partitioning, the partitioning behavior of GFPuv was studied in the presence and absence of LPS. Initially, partitioning of pure GFPuv was investigated at different temperatures, what implies in different excluded-volume effects. Subsequently, GFPuv partitioning was investigated in the presence of $10^7$ EU/mL LPS. The results in terms of GFPuv partition coefficients ($K_{GFPuv}$), mass balances (%$MB_{GFPuv}$), and LPS removal (%$REM_{LPS}$) are reported in Table 1. As shown, %$MB_{GFPuv}$ was close to 100 % in all experiments, demonstrating that GFPuv was stable in the TX-114/buffer micellar system. It is important to note that in some experiments %$MB_{GFPuv}$ was higher than 100 %, which can be related not only with the estimated standard error (10 %) but also with interactions between GFPuv and the nonionic surfactant.

As can also be seen from Table 1b, the percentage of LPS removal was always higher than 98.0 %. Furthermore, the increase of TX-114 concentration and partitioning temperatures led to a higher %$REM_{LPS}$ (98.9 and 99.9 % experiments 11 and 14, respectively). Therefore, the system seems to be efficient for LPS removal from protein preparations.

**Table 1** GFPuv partitioning results in the aqueous two-phase TX-114/buffer micellar system in the presence and absence of LPS

| Assays | TX-114 (wt.%) | $T$ (°C) | EV ($\phi_{bottom}$–$\phi_{top}$) | $R$ | $K_{GFPuv}$ | %$MB_{GFPuv}$ | %$REM_{LPS}$ |
|---|---|---|---|---|---|---|---|
| Pure GFPuv partitioning in ATPMS | | | | | | | |
| 1 | 4.00 | 27.0 | 0.04 | 0.42 | 0.82±0.03 | 99.5±1.2 | |
| 2 | | 29.3 | 0.08 | 0.34 | 0.73±0.03 | 101.0±1.1 | |
| 3 | | 35.0 | 0.17 | 0.29 | 0.53±0.03 | 101.0±1.1 | |
| 4 | | 37.3 | 0.20 | 0.27 | 0.48±0.04 | 102.0±1.5 | |
| 5 | 6.00 | 33.3 | 0.14 | 0.64 | 0.60±0.03 | 99.5±1.2 | |
| 6 | 8.00 | 29.3 | 0.08 | 2.12 | 0.73±0.03 | 99.0±1.2 | |
| 7 | | 37.3 | 0.20 | 0.70 | 0.48±0.03 | 99.8±1.2 | |
| GFPuv partitioning in ATPMS in the presence of LPS | | | | | | | |
| 8 | 4.00 | 27.0 | 0.04 | 0.41 | 0.66±0.03 | 105.00±1.7 | 98.0 |
| 9 | | 29.3 | 0.08 | 0.35 | 0.58±0.04 | 110.00±2.0 | 98.0 |
| 10 | | 35.0 | 0.17 | 0.29 | 0.36±0.04 | 105.00±1.5 | 98.8 |
| 11 | | 37.3 | 0.20 | 0.25 | 0.34±0.03 | 110.00±1.7 | 98.9 |
| 12 | 6.00 | 33.3 | 0.14 | 0.64 | 0.44±0.03 | 99.80±1.2 | 99.7 |
| 12 | 8.00 | 29.3 | 0.08 | 2.13 | 0.58±0.03 | 99.00±1.2 | 98.0 |
| 14 | | 37.3 | 0.20 | 0.68 | 0.34±0.03 | 99.80±1.2 | 99.9 |

The errors represent 95 % confidence levels for the measurements

Legend: *TX-114* the surfactant weight percentual, $\phi_{bottom}$ the surfactant volume fractions in the bottom phase, $\phi_{top}$ the surfactant volume fractions in the top phases, $R$ the volume ratio between the phases of the system, *%$MB_{GFPuv}$* the GFPuv mass balance, *%$REM_{LPS}$* the percentage of LPS removal

## Prediction of GFPuv partition coefficients based on the excluded-volume theory

The partition coefficient values obtained were compared with theoretically calculated ones employing the EV equation proposed by Nikas et al. (1992) (Eq. 2). To apply the equation, the hydrodynamic radius of GFPuv was estimated to be $R_p$=1.87 nm, according to Zimmer (2002). In general, the cross-sectional radius of a cylindrical micelle, $R_0$ (Eq. 2), can be estimated from the optimal length of the surfactant molecule (Puvvada and Blankschtein 1990). Based on this, the estimated $R_0$ value of a TX-114 micelle was 4.0 nm. The EV ($\phi_{bottom}$–$\phi_{top}$) value can be obtained from the experimentally determined coexistence curve for TX-114.

Figure 3 shows a comparison between the experimentally obtained $K_{GFPuv}$ values (diamonds) and the predicted ones, $K_p^{EV}$ (dotted line), as a function of ($\phi_{bottom}$–$\phi_{top}$). As can be seen, reasonable quantitative agreement was observed among the predicted and experimental values. The observed deviation can result from the protein shape. According to the employed model, proteins are approximated as hard spheres. However, GFPuv presents a barrel shape (Zimmer 2002) and, therefore, GFPuv hydrodynamic radius might be slightly overestimated resulting in $K_{GFPuv}$ values lower than the ones predicted by the model.

Figure 4 presents the same comparison between experimentally obtained $K_{GFPuv}$ values and the predicted ones, $K_p^{EV}$, as a function of ($\phi_{bottom}$–$\phi_{top}$) in the presence of LPS. As can be seen, no quantitative agreement was observed between theoretical and experimental partition coefficient values. In the presence of LPS, $K_{GFPuv}$ values were always lower than what is estimated based only in excluded-volume interactions.

In order to investigate the hypothesis of LPS–protein interaction, DLS measurements were performed for pure GFPuv in buffer as well as in the presence of LPS. The results obtained are presented in Fig. 5.

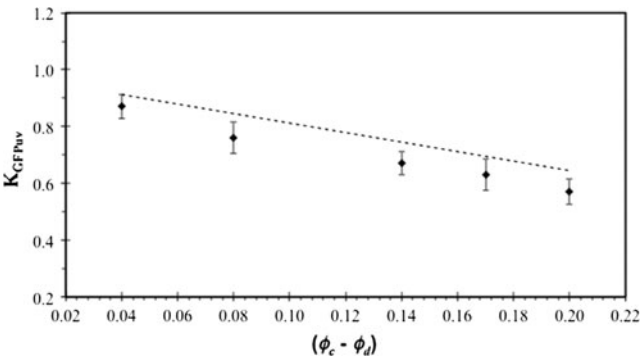


**Fig. 3** Comparison between theoretically predicted (*dotted line*) and experimentally measured (*diamonds*) GFPuv partition coefficients ($K_{GFPuv}$) in the TX-114/buffer micellar system as a function of ($\phi_{bottom}$–$\phi_{top}$), where $\phi_{bottom}$ and $\phi_{top}$ are the TX-114 volume fractions in the bottom and top phases, respectively. The *error bars* represent 95 % confidence levels for the measurements

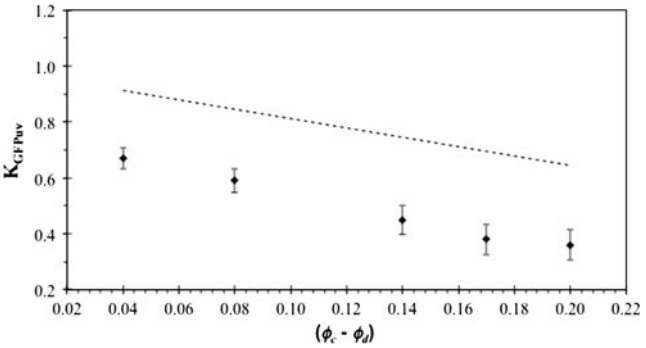


**Fig. 4** Partitioning behavior of GFPuv in the presence of $10^7$ EU/mL of LPS. Comparison between theoretically predicted (*dotted line*) and experimentally measured (*diamonds*) GFPuv partition coefficients ($K_{GFPuv}$) in the TX-114/buffer micellar system as a function of ($\phi_{bottom}$–$\phi_{top}$), where $\phi_{bottom}$ and $\phi_{top}$ are the TX-114 volume fractions in the bottom and top phases, respectively. The *error bars* represent 95 % confidence levels for the measurements

As can be seen in Fig. 5, the DLS results gave support to infer that LPS is inducing GFPuv aggregation. The aggregate diameter increases with the addition of LPS, reaching a plateau at around (LPS)/(GFP)=1.0, corresponding to a 60-nm diameter aggregate (30.0 nm of radius). It is important to point out that according to the DLS measurements the hydrodynamic radius of GFPuv would be approximately 8.0 nm, differing significantly from the $R_p$ value estimated according to Zimmer (2002) (1.87 nm) and used in the theoretical calculations of $K_p^{EV}$.

## Discussion

Our model protein (GFPuv) partitioned preferentially to the top, micelle-poor phase, for all the experiments, $K_{GFPuv}$

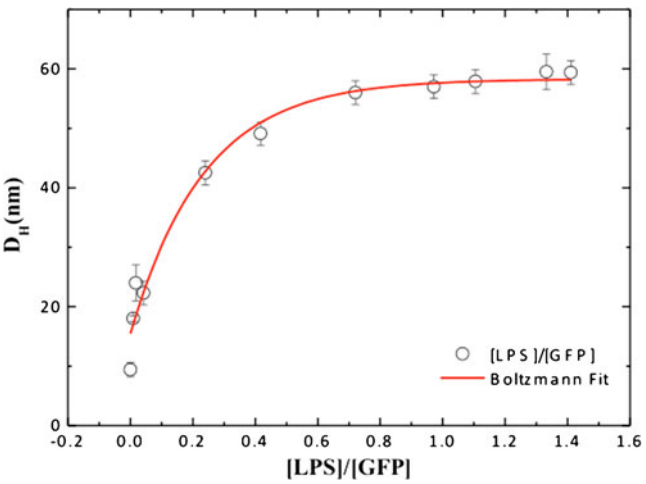


**Fig. 5** Diameter of GFPuv/LPS aggregates ($D_H$) as a function of (LPS)/(GFPuv) ratio, based on DLS measurements. The *error bars* represent 95 % confidence levels for the measurements

values were lower than 1, where it experiences fewer excluded-volume interactions. However, one can note that $K_{GFPuv}$ values were always lower in the presence of LPS (Table 1b). Protein partitioning behavior can be understood from a purely entropic point-of-view since the hydrophilic proteins can sample a larger number of configurations in the micelle-poor phase due to the larger available free volume (Lue and Blankschtein 1996).

Interestingly, LPS was preferentially removed to the bottom phase, allowing depletion of LPS content together with GFPuv, our target molecule. Nonetheless, even removing more than 97 % of the LPS, for highly contaminated preparations the residual LPS concentration could still be high. For example, for a protein originated from a cell lysate with (LPS)=$10^7$ EU/mL, after 99 % LPS removal to the micelle-rich phase of an ATPMS, 100 EU/mL of LPS would still be present. This corresponds to an unacceptable concentration in intravenous products, since the limit set for LPS amounts in human IV preparations is 5.00 EU/kg of body weight/h (US Pharmacopoeia-USP-26 2002). In order to reduce LPS molecules to a tolerable limit, the ATPMS should be processed repeatedly and/or integrated with a process such as affinity chromatography. This approach could ensure high-resolution removal of reminiscent LPS and the achievement of LPS limit concentrations.

The LPS presence influenced the partition results of GFPuv when compared with the predicted by the excluded-volume theory. One can argue that this difference results from the aggregation of LPS in micellar forms altogether with TX-114, due to the amphiphilic nature of both (Fig. 6a, b). In other words, what we would really have are two-phase aqueous mixed micellar systems. This aggregation phenomenon was already observed and described by several authors (Anspach 2001; Lopes et al. 2010). LPS presence in the micelles would result in different shapes and sizes, what in turn could lead to different excluded-volume terms ($\phi_{bottom}$–$\phi_{top}$) and $R_0$ values, for instance. However, considering the concentration of surfactant and LPS present in the investigated systems, one LPS molecule is observed for at least every 740 molecules of TX-114.

It is known that the micellar aggregation number of TX-114 is around 90 (Zdziennicka et al. 2012). On this ground, we can estimate that at each 8 micelles, only one will present an LPS molecule. Thus, most of the micelles remain unaltered in the presence of LPS, once its concentration is much smaller than the TX-114 one. Therefore, it is not reasonable to consider LPS influence in the ATPMS at this concentration, what was already expected based on the identical coexistence curves in the presence and absence of LPS.

One important interaction that was not yet considered for ATPMS is the LPS-protein interaction. This phenomenon was observed by Yuan et al. (1999), which showed nonspecific interactions between LPS and proteins molecules. In our

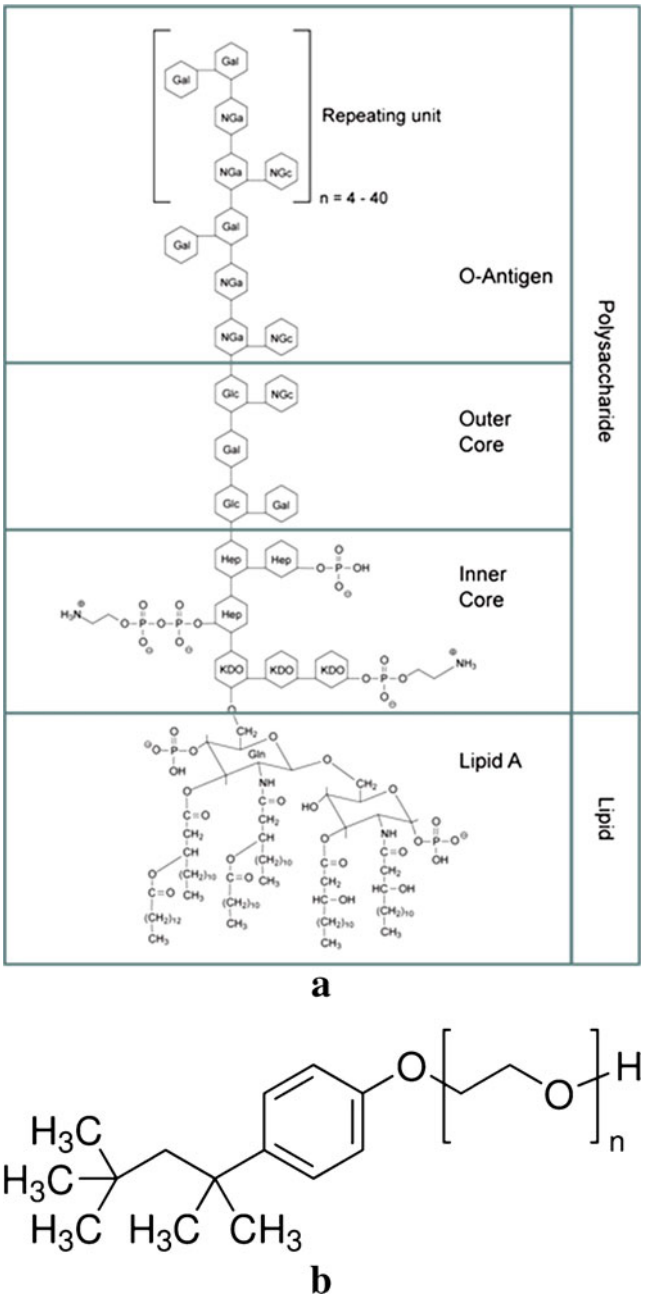


**Fig. 6** **a** General structure for bacterial LPS. Abbreviations: *KDO* 3-deoxy-α-D-mannooctulosonic acid, *Hep* heptulose (ketoheptose), *NGa* galactosamine, *NGc* glucosamine. **b** Nonionic surfactant octylphenol ethoxylate (Triton™ X-114) or *t*-Oct-$C_6H_4$-$(OCH_2CH_2)_n$OH ($n$=7–8)

experiments, based on the concentrations of the system components, we observed a (LPS)/(GFPuv) ratio of 27/1. Therefore, it is possible that protein–LPS interaction leads to the protein–LPS aggregation. Interestingly, such behavior could also explain the observed difference between theoretical and experimental partition coefficient values (see Fig. 4).

However, for the DLS measurements we had to use at least 0.5 mg/mL of GFPuv, in order to get a measurable signal in the DLS detector. Such concentration is 5-fold

higher than the one employed in the ATPMS experiments. Therefore, we believe that protein aggregation by itself is also taking place here and, as a result, the hydrodynamic radius obtained does not correspond to only one protein molecule. In spite of this, it is clear that upon LPS addition it aggregates with proteins increasing the aggregate size and could even promote protein aggregation. If we consider the excluded-volume theory (Eq. 2), $K_p^{EV}$ decreases with the increase in $R_p$. In fact, protein–LPS aggregation would lead to higher hydrodynamic radius values and, since we are not considering the aggregation phenomenon in our theoretical calculations, $K_{GFPuv}$ is always lower than $K_p^{EV}$ in the presence of LPS.

Another argument for the difference observed between theoretical and experimental partition coefficients in the presence of LPS could be the existence of electrostatic interactions. LPS molecules present p$K_1$ and p$K_2$ of 1.3 and 8.2, respectively (Hou and Zaniewski 1990), resulting in an isoelectric point (p*I*) of 4.75. Since the ATPMS investigated presents a pH of 7.20, LPS molecules are bearing a negative charge, similarly to the GFPuv which the p*I* is 5.30 (Bokman and Ward 1981). Therefore, the micelle-rich phase saturated with LPS molecules could promote the electrostatic repulsion of GFPuv to the micelle-poor phase. Nevertheless, as discussed before the (LPS)/(TX-114) ratio is so small that the micelles electrostatic potential cannot be strong enough to influence protein partitioning.

In conclusion, LPS–protein aggregation clearly alters protein partitioning in ATPMS. Our findings may contribute not only to LPS removal from protein preparations by means of ATPMS, but also any aqueous two-phase systems (ATPS). It opens up a question whether employing only ATPS of any kind would be enough to remove LPS to acceptable levels. One possibility would be to employ a purification strategy comprising a final ATPS step based on affinity interactions. Nonetheless, ATPMS can still be considered as an efficient strategy for high loads of LPS removal from protein solutions. One should only keep in mind that, when planning experiments based on the partitioning theories available, it is important to realize that theory might overestimate partition coefficient values due to protein–LPS aggregation. In other words, proteins will be more excluded to the micelle-poor phase than what was estimated by theory but will carry LPS molecules aggregated with them.

**Acknowledgments** This research was supported by grants from the Coordination for Higher Level Graduate Improvements (CAPES/Brazil), National Council for Scientific and Technological Development (CNPq/Brazil), and State of São Paulo Research Foundation (FAPESP/Brazil).

## References

Albertsson PÅ (1986) Partition of cell particles and macromolecules, 3rd edn. Wiley, New York, 346 p

Anspach FB (2001) Endotoxin removal by affinity sorbents. J Biochem Biophys Methods 49:661–681

Bokman SH, Ward WW (1981) Renaturation of Aequorea green fluorescent protein. Biochem Biophsy Res Commun 101:1372–1380

Brömme D, Nallaseth FS, Turk B (2004) Production and activation of recombinant papain-like cysteine proteases. Methods 32:199–206

Chen R (2012) Bacterial expression systems for recombinant protein production: *E. coli* and beyond. Biotechnol Adv 30:1102–1107

Fischer I, Morhardt C, Heissler S, Franzreb M (2012) Partitioning behavior of silica-coated nanoparticles in aqueous micellar two-phase systems: evidence for an adsorption-driven mechanism from QCM-D and ATR-FTIR measurements. Langmuir 28:15789–15796

Gupta R, Gupta N, Rathi P (2004) Bacterial lipases: an overview of production, purification and biochemical properties. Appl Microbiol Biotechnol 64:763–781

Hou KC, Zaniewski R (1990) Depyrigenation by endotoxin removal with positively charged depth filter cartridge. J Parenter Sci Technol 44:204–209

Kamei DT, Wang DIC, Blankschtein D (2002) Fundamental investigation of protein partitioning in two-phase aqueous mixed (nonionic/ionic) micellar systems. Langmuir 18:3047–3057

Liu CL, Nikas YJ, Blankschtein D (1996) Novel bioseparations using two-phase aqueous micellar systems. Biotechnol Bioeng 52:185–192

Lopes AM, Rangel-Yagui CO, Pessoa-Jr A (2008) Can affinity interactions influence the partitioning of glucose-6-phosphate dehydrogenase in two-phase aqueous micellar systems? Quím Nova 31:998–1003

Lopes AM, Magalhães PO, Mazzola PG, Rangel-Yagui CO, Carvalho JCM, Penna TCV, Pessoa-Jr A (2010) LPS removal from an *E. coli* fermentation broth using aqueous two-phase micellar system. Biotechnol Prog 26:1644–1653

Lopes AM, Magalhães PO, Mazzola PG, Rangel-Yagui CO, Carvalho JCM, Penna TCV, Pessoa-Jr A (2011) Green fluorescent protein extraction and LPS removal from *E. coli* fermentation medium using aqueous two-phase micellar system. Sep Purif Technol 81:339–346

Lopes AM, Romeu JS, Perera GM, Paez R, Morales RP, Pessoa-JR A, Cardenas LZ (2012) Adsorption of endotoxins on IDA-Ca2+ by ion metal affinity chromatography. Chin J Chromatogr 30:1194–1202

Lue L, Blankschtein D (1996) A liquid-state theory approach to modeling solute partitioning in phase-separated solutions. Ind Eng Chem Res 35:3032–3043

Magalhães PO, Lopes AM, Mazzola PG, Rangel-Yagui CO, Penna TCV, Pessoa-Jr A (2007) Methods of endotoxin removal from biological preparations: a review. J Pharm Pharm Sci 10:271–287

Mazzola PG, Lam H, Kavoosi M, Haynes CA, Pessoa-Jr A, Penna TCV, Haynes CA, Wang DIC, Blankschtein D (2006) Affinity-tagged green fluorescent protein (GFPuv) extraction from a clarified *E. coli* cell lysate using a two-phase aqueous micellar system. Biotechnol Bioeng 93:998–1004

Mazzola PG, Lopes AM, Hasmann FA, Jozala AF, Penna TCV, Magalhaes PO, Rangel-Yagui CO, Pessoa-Jr A (2008) Liquid–liquid extraction of biomolecules: an overview and update of the main techniques. J Chem Technol Biot 83:143–157

Nikas YJ, Liu CL, Srivastava T, Abbott NL, Blankschtein D (1992) Protein partitioning in two-phase aqueous nonionic micellar solutions. Macromolecules 25:4794–4806

Primrose SB, Twyman R (2006) Principles of gene manipulation and genomics. Wiley-Blackwell, New York, 672 p

Puvvada S, Blankschtein D (1990) Molecular-thermodynamic approach to predict micellization, phase behavior, and phase separation of micellar solutions. I. Application to nonionic surfactants approach. J Chem Phys 92:3710–3724

Rangel-Yagui CO, Lam H, Kamei DT, Wang D, Pessoa-Jr A, Blankschtein D (2003) Glucose-6-phosphate dehydrogenase partitioning in two-phase aqueous mixed (nonioc/cationic) micellar systems. Biotechnol Bioeng 82:445–456

Terpe K (2006) Overview of bacterial expression systems for heterologous protein production: from molecular and biochemical fundamentals to commercial systems. Appl Microbiol Biotechnol 72:211–222

US Pharmacopoeia-USP-26 (2002). US Pharmacopeial Convention, Rockville, 2569 p

US Pharmacopeia and National Formulary-USP-24-NF-19 (2000) Bacterial endotoxins. Test. Supplement 85:2875–2879

Westphal O, Jann K (1965) Bacterial lipopolysaccharides: extraction with phenol-water and further applications of the procedure. Methods Carbohydr Chem 5:83–91

Yuan A, Pardy RL, Chia CP (1999) Nonspecific interactions alter lipopolysaccharide patterns and protein mobility on sodium dodecyl sulfate polyacrylamide gels. Electrophoresis 20:1946–1949

Zdziennicka A, Szymczyk K, Krawczyk J, Jańczuk B (2012) Critical micelle concentration of some surfactants and thermodynamic parameters of their micellization. Fluid Phase Equilib 322–323:126–134

Zimmer M (2002) Green fluorescent protein (GFP): applications, structure, and related photophysical behavior. Chem Rev 102:759–781